

Structural and Tensile Properties of Self-Assembled DNA Network on Mica Surface

Itsuo Hanasaki, Hirofumi Shintaku, Satoshi Matsunami
Satoyuki Kawano¹

Abstract: Self-assembly is one of the physical phenomena that are promising for the manufacturing process of the devices on which DNA molecules are mounted as the components. We have conducted a structural study of self-assembled poly(dA)·poly(dT) DNA networks on mica surface to discuss the design requirements. The results indicate that the network formation process consists of the adsorption and the subsequent coarsening. The final form of the component filaments are roughly straight. These characteristics imply the possible tensile loads during the network formation. Therefore, we have conducted molecular dynamics simulations of tensile tests of a short DNA fragment to elucidate the relevant mechanical properties. The effective tensile properties strongly depend on the loading condition of the clamp, which can affect the functionality of the molecules.

Keywords: DNA, substrate, self-assembly, network structure, biodevice, molecular dynamics

1 Introduction

DNA is not only important in biology but also in engineering. They are expected to be the components of nanoscale structures [Goodman, Schaap, Tardin, Erben, Berry, Schmidt, and Turberfield (2005)] and electronic devices [Terawaki, Otsuka, Lee, Matsumoto, Tanaka, and Kawai (2005)] because of the unique properties [Kawano and Maruyama (2005); Maruyama, Tachikawa, and Kawano (2005); Shimizu, Kawano, and Tachikawa (2006)]. They may also be utilized as templates for nano-devices [Maeda, Tabata, and Kawai (2001)]. One of the fundamental issues concerning such industrial applications is how to assemble them efficiently so that they actually function as the devices. It has been reported that DNA molecules form network patterns when their aqueous solutions are dried on inorganic substrates

¹ Department of Mechanical Science and Bioengineering, Graduate School of Engineering Science, Osaka University, Machikaneyama-cho 1-3, Toyonaka, Osaka 560-8531, Japan

[Kanno, Tanaka, Miyoshi, and Kawai (2000a,b); Tanaka, Maeda, Cai, Tabata, and Kawai (2001); Tanaka, Cai, Tabata, and Kawai (2001); Wu, Li, and Wang (2004); Kawano (2005)]. Such self-assembly may be used as an efficient manufacturing process in combination with others. Manipulation of molecules [Nagahiro, Kawano, and Kotera (2007); Hanasaki, Takahashi, Sazaki, Nakajima, and Kawano (2008); Hanasaki, Nakamura, Yonebayashi, and Kawano (2008); Hanasaki, Yonebayashi, and Kawano (2009)] as well as cells and tissues [Shintaku, Kuwabara, Kawano, Suzuki, Kanno, and Kotera (2007); Shintaku, Okitsu, Kawano, Matsumoto, Suzuki, Kanno, and Kotera (2008)] through fluid dynamics is often discussed in recent years. In this study, we have conducted experiments of the DNA network formation on mica substrates, and analyzed the obtained structures. In particular, we focus on the time evolution of the network structure. As will be shown later, the formation of network structure is not simply an adsorption process. There exists two main mechanisms: the adsorption and the coarsening. Variation of the solution exposure time for an appropriate range of period reveals the transition of dominant mechanism in the course of the network formation.

The final network structure consists of filaments. The filaments consists of multiple DNA molecules, and many of the filaments are longer than the constituent DNA molecules. Nevertheless, the filaments are more or less straight and the branches with three or four junctions are formed. This implies that the filaments are not completely in a mechanically loose state. Since the DNA network filaments are longer and wider than the constituent molecules and they have junctions in various directions, there can be several types of tensile load that the molecules may experience in the network formation process. Although the direct measurement provides the structural information of the network level, it does not have a resolution of that of each molecule in detail. The structures of biomolecules are essential for their unique functionalities. Therefore, we have also conducted molecular dynamics (MD) simulations of tensile tests for a DNA fragment to examine the relevant mechanical properties. The elastic properties of DNA have been studied both experimentally and theoretically so far (cf. Ref. [Bustamante, Smith, Liphardt, and Smith (2000)] for reviews). In fact, DNA is one of the typical materials that has been regarded as promising for nanotechnology applications [Srivastava and Atluri (2002)]. However, the reported studies have been focused on the molecules longer than its persistence length due to the importance in the biological context [Bustamante, Bryant, and Smith (2003)]. In this article, we focus on the tensile properties that are more closely related to the network structures and the design of artificial devices. In contrast with *in vivo* situations where the DNA molecules are solved in a solvent, the configurations of the molecules is often desired to be partly fixed for the industrial applications. We investigate the influence of clamp conditions on

the tensile properties. The results indicate the clear difference of measured tensile properties for the different conditions.

2 Formation of network structures on the substrates

We solvated 50-bp poly(dA)·poly(dT) DNA fragments (Bex, Japan) in pure water at the concentration of 80 $\mu\text{g}/\text{ml}$. Several factors can be considered to play some roles in the formation of the network structure. For example, the concentration of the DNA fragments [Kawano (2005)] and the ionic strength of the solution could significantly affect the geometry of the final structure. However, we focus on the basic properties upon the time evolution, which is examined by the variation of the solution exposure time. The water had been sterilized in the autoclave at 394 K for 20 minutes. The prepared aqueous solution of the DNA was then stirred for 2 hours and was kept at 278 K for 12 hours. The 5 μl of the solution was dropped and spread on mica (MICA, For Atomic Scale Calibration, Digital Instruments, Veeco Metrology Group) substrates of 6 mm on a side. The surface layers of the mica substrate had been cleaved to obtain the clean surface. The temperature was kept at 300 K. The solution was kept under this condition for different exposure time to examine the influence on the structures. Finally, the solution was blown off using N_2 gas. After 1 hour, the substrate surface was observed using the dynamic force mode (DFM) of the atomic force microscope (AFM)(SPI4000-SPA400,SII). Thus, we do not wash the substrate after the adsorption process as we intend to capture the snapshots of the network formation process without affecting the structure. The use of pure water instead of buffer solution has an advantage to avoid unclear AFM images due to the solutes remaining on the substrate when the washing procedure is absent.

The samples of the observed AFM images of self-assembled DNA networks with different exposure time to the aqueous solutions are shown in Fig.1. The time is counted from when the solution is dropped on a substrate. The bright area indicates the DNA fragments on the substrate. It can be seen that the DNA fragments are connected with each other in the length direction since the fragment is 50 bp \cong 1.7 nm for B type DNA. Three samples are shown for each exposure time. Since pure water is used as the solvent, the surface condition of the mica may be easily changed by the adsorption. However, the formation process of the DNA network is reproducible. The freshly cleaved mica surface is likely to contain cations such as K^+ [Sides, Faruqui, and Gellman (2009)], and they can be the sources of attractive interaction between the DNA fragments and substrate surface.

The DNA fragments show relatively uniform adsorption on the substrate for the shorter exposure time (Fig.1 (i)-(iii)). No significant difference in terms of the structure is found from 6.0×10^{-1} s to 6.0×10^2 s. On the other hand, the exposure

time longer than 6.0×10^2 s leads to the network structures (Fig.1(iv)). The network appears to coarsen with increasing exposure time (Fig.1(v)). It can be seen that the filaments widen and the network size grows. These results indicate that the network formation process consists of two stages: the adsorption and the coarsening.

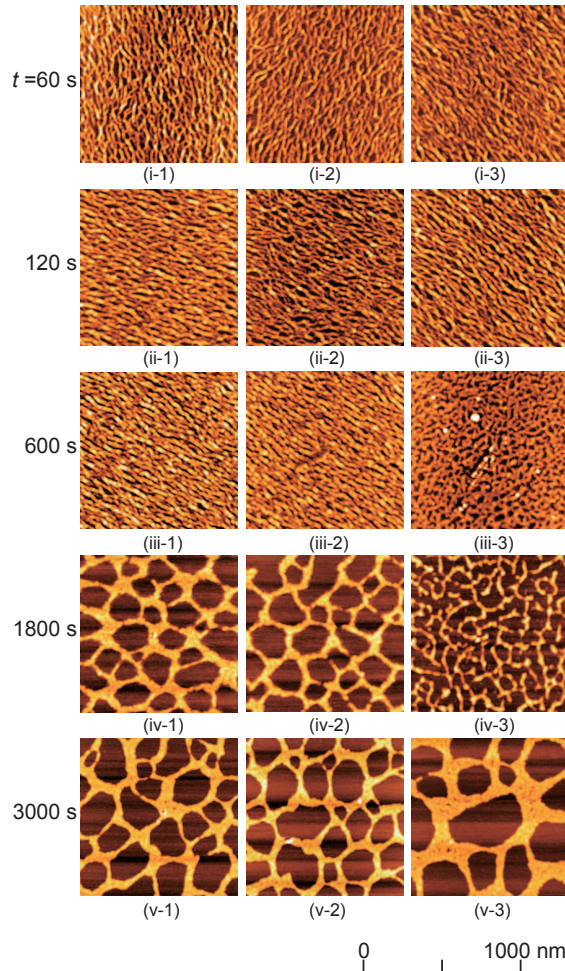


Figure 1: AFM images of the self-assembled DNA network on mica surface with different exposure time to the solutions at (i) 6.0×10^2 s, (ii) 1.2×10^3 s, (iii) 6.0×10^3 s, (iv) 1.8×10^3 s, and (v) 3.0×10^3 s. The three images for each exposure time are obtained from different trials under the same conditions.

The height spectra of Fig.1(ii-2) and (iv-2) are shown in Fig.2 (a) and (b), respectively. The height spreads widely during the adsorption. On the other hand, the dis-

tribution has a clear peak at 0.52 nm and another at 1.86 nm at the coarsening stage. The first peak corresponds to the surface of the mica substrate, and the second one corresponds to the mean height of the DNA network. It is not clear whether the DNA fragments remain double-stranded or become single strands after the network formation. In fact, it is generally difficult to distinguish them only from the height data as shown in Fig.2 [Hansma, Sinsheimer, Li, and Hansma (1992)]. Fig.2(c) shows the volume of the adsorbed DNA molecules estimated from the height data. There is a difference between the trends of the volume evolution for the exposure times shorter and longer than 6.0×10^2 s. When shorter than 6.0×10^2 s, the volume looks increasing with the exposure time. In contrast, it decreases when longer than that. The adsorption appears to be saturated at 6.0×10^2 s. This time scale can be interpreted as that of diffusion-limited transport phenomena. It is inferred to be $h^2/D \sim O(10^2)$ s from a thickness $h \sim O(10^{-4})$ m of the solution on the substrate and the diffusion coefficient $D \sim O(10^{-10})$ m²/s of the DNA fragments. This implies that the additional adsorption is not significant in the process of coarsening. The decrease after 6.0×10^2 s is likely to be caused by the volume shrinking because of the similarity with the network formation of protein molecules from uniformly distributed structure [Tanaka and Nishikawa (2005)]. Therefore, some parts of the structure can be considered to experience tensile loads upon network formation and they are stretched into filaments. The branches with three or four junctions are formed where the tension exists in the multiple directions. The process of the network formation depends on the competition between the adsorption of DNA fragments on the mica surface and the coarsening due to volume shrinking. It can be interpreted that the transition observed here takes place when the coarsening becomes dominant. While there has been several experimental works on the DNA network formation, the time evolution had not been studied. The direct measurement using e.g., AFM is likely to affect the dynamics and the unperturbed dynamics has been out of reach. Therefore, we indirectly measured the dynamics by the variation of the solution exposure time, based on the high reproducibility of the phenomena.

In order to evaluate the coarsening process quantitatively, we calculated the two-dimensional Fourier transform of the height distribution. Fig.3 shows the wavelength variation obtained from the spectral data. Fig.3 (a) and (b) correspond to Fig.1 (ii-2) and (iv-2), respectively. The distribution is roughly log normal, which has the longer tail at the long-wavelength part and the median value larger than the modal one. This distribution implies that the growth of the filaments is caused by the coalescence, while not by the Ostwald ripening process [Limary and Green (2002)]. We define the geometric mean value L of the wavelength as the characteristic scale of the network structure as it reflects the widths of the network filaments.

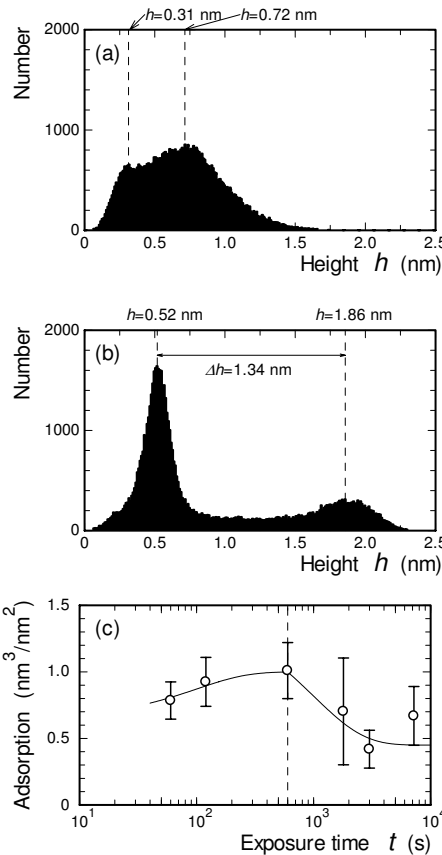


Figure 2: Height distributions (a) and (b) obtained from the AFM images of Fig.1 (ii-2) and (iv-2), respectively. (c) Volume of adsorbed DNA molecules per 1 nm^2 for various exposure times.

Fig.4 shows L as a function of the exposure time. It is almost constant around 35–45 nm with the shorter exposure time up to 6.0×10^2 s, and increases when longer than that. This corresponds to the coarsening of the network structure. The time point of transition agrees with that in Fig.2 (c). L grows as t^α with $\alpha=0.63$ in the coarsening process. This trend implies that the coarsening is not caused by the Ostwald ripening process whose exponent is 1/3 [Limary and Green (2002)]. Since the extra adsorption is not significant in the coarsening, the origin of filament widening is mainly attributed to the coalescence of the adsorbed molecules.

As the network structures look self-similar [Kawano (2005)], we have also measured the fractal dimension of the binarized AFM images of the network structures

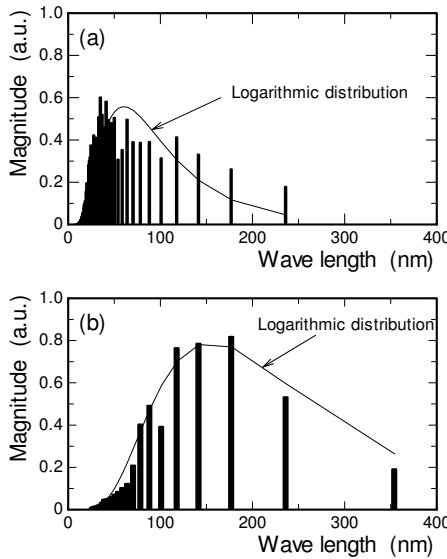


Figure 3: Distribution of wavelength obtained from the AFM images: (a) and (b) correspond to Fig.1(ii-2) and (iv-2), respectively. Bars and solid lines indicate experimental data and log-normal distribution fitted to the experiment, respectively.

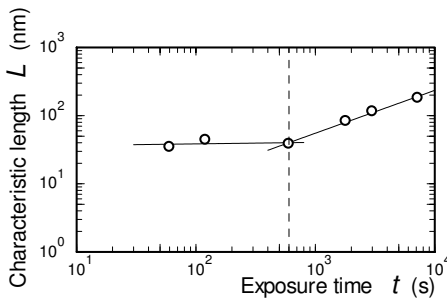


Figure 4: Characteristic length as a function of exposure time. Circles indicated the experimental result. Solid lines indicate the fitting $L \sim t^\alpha$ with $\alpha=0.022$ and 0.63 for the first and second stages of the process, respectively.

using the box-counting method [Kawano (2005)]. The object of interest is covered by the (generalized) boxes having size of r , then the number of boxes that include the object of interest is counted. When the number of boxes is n , the corresponding

fractal dimension is obtained from

$$D_f = -\lim_{r \rightarrow 0} \frac{\log n(r)}{\log r}. \quad (1)$$

In practice, D_f is calculated from the linear approximation of $\log n(r)/\log r$. D_f of the DNA network structure in the AFM image is shown in Fig.5 as a function of the exposure time. D_f is 1.75-1.90 up to 6.0×10^2 s and it reduces to be about 1.66 during the coarsening process. This measurement also indicates the transition at 6.0×10^2 s. D_f is constant beyond 3.0×10^3 s, indicative of an equilibrium state. The asymptotic value is close to that of the diffusion-limited aggregation (DLA) [Witten and Sander (1981)] pattern. The fractal dimension of the latter in the two dimensional space is 1.7 [Tolman and Meakin (1989)]. This slight difference may have been caused by the rearrangement of the filaments due to the coalescence and stretching.

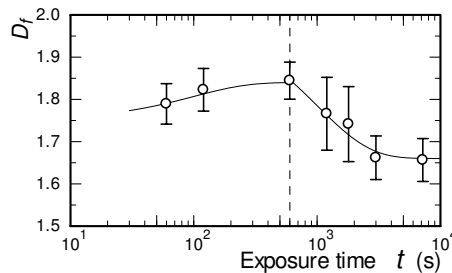


Figure 5: Fractal dimension of the DNA network structure as a function of exposure time to the solution.

3 Effects of tensile loads on the molecular structure

As described in the previous section, DNA network is formed from the uniformly distributed state through volume shrinking. The cations adhered on the substrate surface may play a role of anchors to keep some points of DNA fragments at specific sites. The obtained structures have more or less straight branches with three or four junctions, and they are longer than a DNA fragment as shown in Fig.1. Thus, the tensile properties of the DNA network can play an important role in defining the final structure. However, the direct measurement employed here does not provide the information of this resolution. Therefore, we examine the influence of the load conditions on the tensile properties of a short DNA molecule using steered molecular dynamics (SMD) simulations [Sotomayor and Schulten (2007); Hanasaki, Haga, and Kawano (2008)]. Although the concept of SMD, especially for biomolecules,

is relatively new, MD has been used for the mechanics of solids (e.g., [Kitagawa, Nakatani, and Shibutani (1994)] [Nishimura and Miyazaki (2001)] [Matsumoto, Nakagaki, Nakatani, and Kitagawa (2005)] [Matsumoto and Nakagaki (2005)]).

Equations of motion are solved for the atoms that consist the system of interest. The SMD is a kind of MD where the guiding external potential is introduced to analyze the response of the system. We use the AMBER9 program package[Case, Darden, III, Simmerling, Wang, Duke, Luo, Merz, Pearlman, Crawley, Walker, Zhang, Wang, Hayik, Roitberg, Seabra, Wong, Paesani, Wu, Brozell, Tsui, Gohlke, Yang, Tan, Mongan, Hornak, Cui, Beroza, Mathews, Schafmeister, Ross, and Kollman (2006)] to conduct the SMD simulations here. The AMBER ff03 force field[Duan, Wu, Chowdhury, Lee, Xiong, Zhang, Yang, Cieplak, Luo, and Lee (2003); Lee and Duan (2004)] is employed for the interatomic potential, and generalized Born model[Onufriev, Bashford, and Case (2004)] is used for solvent description. A cut-off distance of 1.2 nm is used for the calculation of the nonbonded interactions. The Langevin thermostat is applied with a collision frequency parameter of 1 ps^{-1} to keep the temperature at 300 K. The equations of motion are solved using the leap-frog algorithm with a time step of 2 fs. We numerically conducted the tensile tests of the 10-bp poly(dA)·poly(dT) DNA. The specimen is equilibrated in advance by 100 ps of MD after 500 steps of energy minimization. The energy minimization consists of 250 steps of the conjugate gradient method following 250 steps of the steepest decent method, starting from the initial configuration generated by the program nucgen in the AMBER9. The tensile test under each condition is conducted for five different microscopic initial configurations obtained from further equilibrations having 100 ps interval between each configuration. The results presented are the ensemble average of the five tests except for the snapshots shown later. In order to apply the tensile loads, a harmonic spring potential is applied between the ends of the specimen with a spring constant of 5 kcal/mol· \AA^2 with a time-dependent natural length increasing at a rate of 5 m/s starting from the equilibrated DNA length. The specification of the conditions is schematically shown in Fig.6. The distance between the center of mass of C5' atom of adenine and C3' atom of thymine, and that of C3' atom of adenine and C5' atom of thymine is increased in case 1. The distance between C5' atom of thymine and C3' atom of thymine is increased in case 2. The distance between C5' atom of adenine and C3' atom of adenine is increased in case 3. The distance between C5' atom of adenine and C3' atom of thymine is increased in case 4.

The obtained force-extension properties are shown in Fig.7. The extension is shown as the end-to-end distance of the specimen normalized by the contour length of 3.4 nm. Thus, the value 1.0 means the zero extension. Case 1 is the standard condition to be compared with other cases as it satisfies the conditions that the

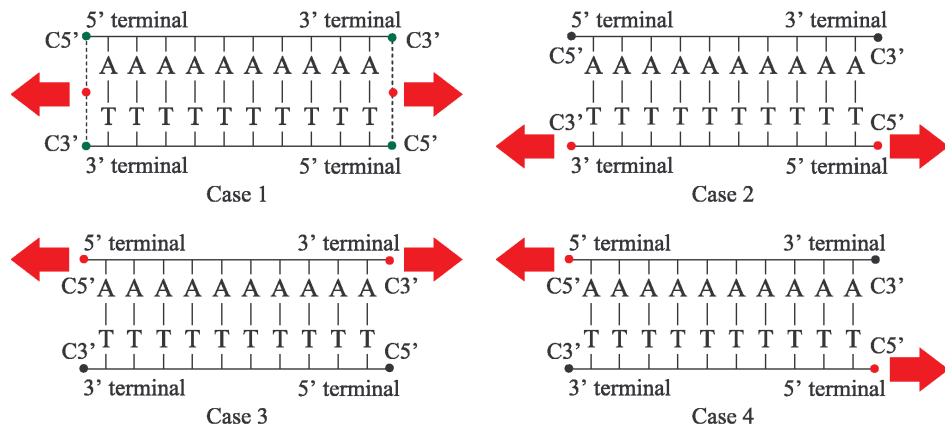


Figure 6: Schematic view of the loading conditions in the SMD. Although the DNA is illustrated as a ladder structure for clarity, it has a structure of double helix after the equilibration before the tensile tests.

pulling direction is the axis of double helix and both of the strands are pulled. The force-extension characteristics consist of two regimes: the tensile property changes at the end-to-end distance of about 1.6. The helical structure is unwound in the regime of the distance less than that. This can be confirmed qualitatively by the sequential snapshots Fig.8 for one of the trials in case 1. The visualization of the molecules are conducted using VMD[Humphrey, Dalke, and Schulten (1996)]. The transition of the state is confirmed quantitatively by the change of torsional angle of the helix as shown in Fig.9. The time-evolution of the representative inter-atomic distances of the DNA backbone for case 1 is shown in Fig.10. P-O', C'-C' and C'-O' indicate phosphorous-oxygen, carbon-carbon and carbon-oxygen, respectively. They do not change until the double helix is unwound, and starts growing after that without clear starting point. The force where the tensile property changes is close to the force necessary for overstretching transition and melting 35 pN of poly(dA-dT) DNA[Rief, Clausen-Schaumann, and Gaub (1999)]. Some researchers distinguish between overstretching transition (or B-S transition) and melting transition, but it has recently been suggested that the former is rather a kind of melting transition than a well-defined configurational change[Harris, Sands, and Laughton (2005)].

The cases 2 and 3 show similar properties. For end-to-end distance substantially larger than 1.6, the force value and slope of the curve are about half of those in case 1. Furthermore, it holds also for the regime of the end-to-end distance smaller than 1.6. Only one of the two strands is clamped and directly pulled in the cases 2 and 3. Thus, the interactions between the two constituent strands do not necessarily lead

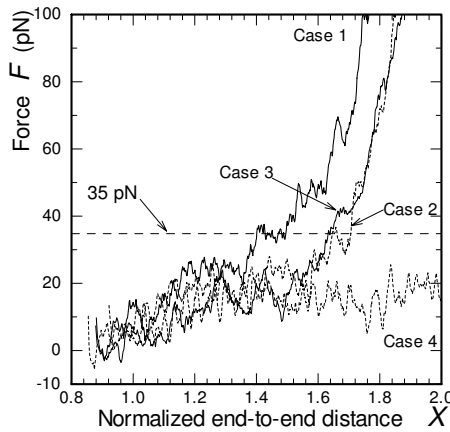


Figure 7: Tensile properties of the 10-bp poly(dA)·poly(dT) DNA fragment under different conditions of the loading.

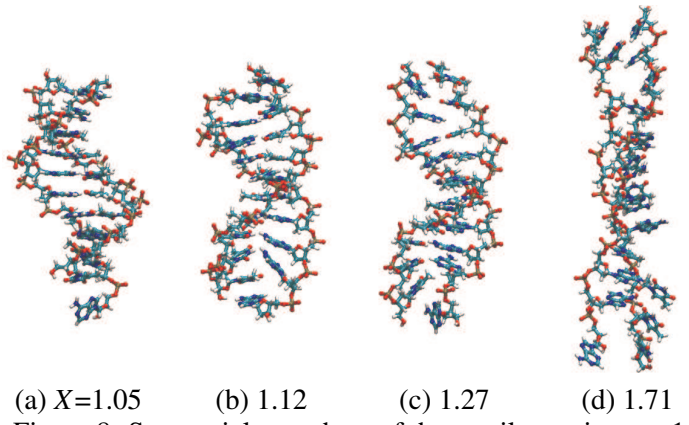


Figure 8: Sequential snapshots of the tensile test in case 1.

to the same tensile strength when only one of the two strands is directly stretched. Indeed, this force-extension property is rather close to that of single-stranded DNA molecule shown in Fig.1b of Ref.[Bustamante, Bryant, and Smith (2003)]. In case 4, the force-extension property is clearly different from other cases. The obtained force is less than 30 pN even for the end-to-end distance substantially larger than 1.6. This is because the clamp condition is assigned in such a way that the adenine strand is pulled at the one end and the thymine strand is pulled at the other end. Such conditions lead to the unwinding and consequently the unbinding effect much larger than other cases. It has been reported that the necessary force to unzip the

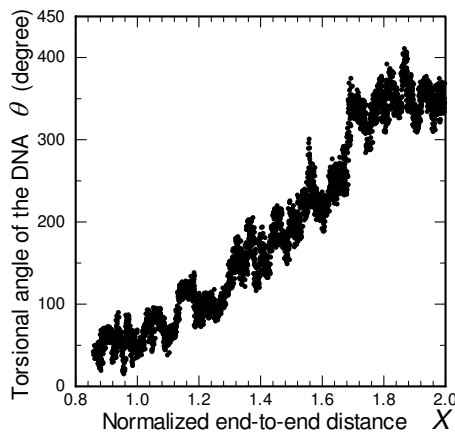


Figure 9: Torsional angle of the 10-bp poly(dA)·poly(dT) DNA fragment under the tensile condition of case 1.

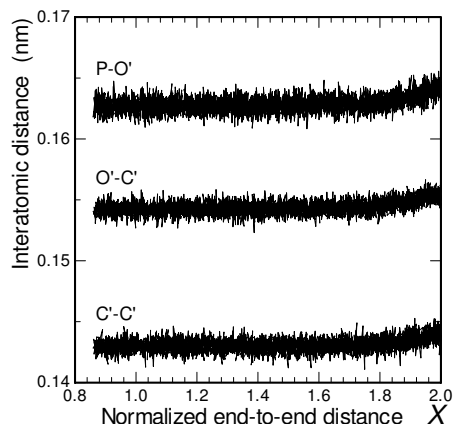


Figure 10: Interatomic distances of the backbone for 10-bp poly(dA)·poly(dT) DNA fragment under the tensile condition of case 1. The values are the averages for different residues.

base pair of adenine-thymine is about 10 pN[Essevaz-Roulet, Bockelmann, and Heslot (1997)], which is smaller than the force necessary for the B-S transition of poly(dA-dT) DNA[Rief, Clausen-Schaumann, and Gaub (1999)].

The structure of biomolecules are generally essential for their functionalities. If it is different from that of *in vivo* state, some properties of the DNA can be different. The numerical tensile tests suggest that the double-stranded DNA fragments can

be over-stretched if the tensile load exceeds tens of pN. The experimental results obtained here does not provide the information about the magnitude of such forces. However, the peak in the height distribution of the network had about 2 nm from the substrate as shown in Fig.2 and as observed in our previous experiment[Kawano (2005)]. This suggests that many of the DNA fragments kept double-stranded after the network formation while further study is necessary for concluding it. Thus, the currently available data indicate that the tensile loads upon network formation is lower than tens of pN although the DNA fragments undergo volume shrinking. When the thermodynamic or other conditions of the self-assembly is varied to tune the characteristics of the network structure for a specific device, tensile strength of the molecules and the load will change. The design of DNA devices employing the network structure needs to meet these conditions for specification.

4 Concluding remarks

The utilization of self-assembly enables the simple process for the production of molecular patterns. In this article, self-assembled DNA network patterns are experimentally produced and analyzed. The fractal dimension of the DNA network is close to that of the two-dimensional diffusion-limited aggregation pattern. Since the diffusion process is stochastic at the level of each molecule, the principle of the control of such process should be different from that of macroscopic objects. As a first step, we have shown the dependence of the exposure time of the substrate to the solution, i.e., the macroscopic condition that can be tuned more easily compared to the microscopic ones. The result indicates the existence of the optimum exposure time for the well-defined network structure, and that the network formation consists of the adsorption and coarsening processes.

The obtained structure is not so regular as the existing macroscopic artificial devices. However, there will be some situations where such conventional regularity might not be necessary, e.g., for certain kinds of sensing devices. In addition, the manufacturing of the conventional devices also rely on various processes in reality. Thus, the network formation by self-assembly may also be used for preliminary process before more specific, artificial process by single-molecule manipulation technologies. The link with existing technologies often calls for well-defined structure. The results of numerical tensile tests of short DNA molecules shows the significance of clamp conditions on the effective tensile properties, and the necessity of different viewpoint from biological context when the DNA is to be used for artificial devices in the near future.

References

- Bustamante, C.; Bryant, Z.; Smith, S. B.** (2003): Ten years of tension: single-molecule DNA. *Nature*, vol. 421, pp. 423–427.
- Bustamante, C.; Smith, S. B.; Liphardt, J.; Smith, D.** (2000): Single-molecule studies of DNA mechanics. *Curr. Opin. Struct. Biol.*, vol. 10, pp. 279–285.
- Case, D. A.; Darden, T. A.; III, T. E. C.; Simmerling, C. L.; Wang, J.; Duke, R. E.; Luo, R.; Merz, K. M.; Pearlman, D. A.; Crawley, M.; Walker, R. C.; Zhang, W.; Wang, B.; Hayik, S.; Roitberg, A.; Seabra, G.; Wong, K. F.; Pae-sani, F.; Wu, X.; Brozell, S.; Tsui, V.; Gohlke, H.; Yang, L.; Tan, C.; Mongan, J.; Hornak, V.; Cui, G.; Beroza, P.; Mathews, D. H.; Schafmeister, C.; Ross, W. S.; Kollman, P. A.** (2006): Amber9.
- Duan, Y.; Wu, C.; Chowdhury, S.; Lee, M. C.; Xiong, G.; Zhang, W.; Yang, R.; Cieplak, P.; Luo, R.; Lee, T.** (2003): A point-charge force field for molecular mechanics simulations of proteins based on condensed-phase quantum mechanical calculations. *J. Comp. Chem.*, vol. 24, pp. 1999–2012.
- Essevaz-Roulet, B.; Bockelmann, U.; Heslot, F.** (1997): Mechanical separation of the complementary strands of DNA. *Proc. Nat. Acad. Sci.*, vol. 94, pp. 11935–11940.
- Goodman, R. P.; Schaap, I. A. T.; Tardin, C. F.; Erben, C. M.; Berry, R. M.; Schmidt, C. F.; Turberfield, A. J.** (2005): Rapid chiral assembly of rigid DNA building blocks for molecular nanofabrication. *Science*, vol. 310, pp. 1661–1665.
- Hanasaki, I.; Haga, T.; Kawano, S.** (2008): Antigen-antibody unbinding process through steered molecular dynamics of a complex of fv fragment and lysozyme. *J. Phys.: Condens. Matter*, vol. 20, pp. 255238 (10 pages).
- Hanasaki, I.; Nakamura, A.; Yonebayashi, T.; Kawano, S.** (2008): Structure and stability of water chain in a carbon nanotube. *J. Phys.: Condens. Matter*, vol. 20, pp. 015213.
- Hanasaki, I.; Takahashi, H.; Sasaki, G.; Nakajima, K.; Kawano, S.** (2008): Single-molecule measurements and dynamical simulations of protein molecules near silicon substrates. *J. Phys. D: Appl. Phys.*, vol. 41, pp. 095301.
- Hanasaki, I.; Yonebayashi, T.; Kawano, S.** (2009): Molecular dynamics of a water jet from a carbon nanotube. *Phys. Rev. E*, vol. 79, pp. 046307.

- Hansma, H. G.; Sinsheimer, R. L.; Li, M. Q.; Hansma, P. K.** (1992): Atomic force microscopy of single-and double-stranded dna. *Nucleic Acids Research*, vol. 20, pp. 3585–3590.
- Harris, S. A.; Sands, Z. A.; Laughton, C. A.** (2005): Molecular dynamics simulations of duplex stretching reveal the importance of entropy in determining the biomechanical properties of DNA. *Biophys. J.*, vol. 88, pp. 1684–1691.
- Humphrey, W.; Dalke, A.; Schulten, K.** (1996): *J. Mol. Graphics*, vol. 14, pp. 33.
- Kanno, T.; Tanaka, H.; Miyoshi, N.; Kawai, T.** (2000): Formation and control of two-dimensional deoxyribonucleic acid network. *Appl. Phys. Lett.*, vol. 77, pp. 3848–3850.
- Kanno, T.; Tanaka, H.; Miyoshi, N.; Kawai, T.** (2000): A new self-fabrication of large-scale deoxyribonucleic acid network on mica surfaces. *Jpn. J. Appl. Phys.*, vol. 39, pp. L269–L270.
- Kawano, S.** (2005): Fractal dimension analysis in self-assembled poly(dA)·poly(dT) DNA network on mica surface. *JSME. Int. J., Ser. B*, vol. 48, pp. 191–195.
- Kawano, S.; Maruyama, Y.** (2005): Mathematical model for polaronic effects of charge transport in DNA. *JSME. Int. J., Ser. B*, vol. 48, pp. 456–463.
- Kitagawa, H.; Nakatani, A.; Shibutani, Y.** (1994): Molecular dynamics study of crack processes associated with dislocation nucleated at the tip. *Materials Science and Engineering*, vol. A176, pp. 263.
- Lee, M. C.; Duan, Y.** (2004): Distinguish protein decoys by using a scoring function based on a new amber force field, short molecular dynamics simulations, and the generalized born solvent model. *Proteins*, vol. 55, pp. 620–634.
- Limary, R.; Green, P. F.** (2002): Late-stage coarsening of an unstable structured liquid film. *Phys. Rev. E*, vol. 66, pp. 021601(6 pages).
- Maeda, Y.; Tabata, H.; Kawai, T.** (2001): Two-dimensional assembly of gold nanoparticles with a DNA network template. *Appl. Phys. Lett.*, vol. 79, pp. 1181–1183.
- Maruyama, Y.; Tachikawa, M.; Kawano, S.** (2005): Ab initio study of DNA double-strand breaks by hydroxyl radical. *JSME. Int. J., Ser. B*, vol. 48, pp. 196–201.

Matsumoto, R.; Nakagaki, M. (2005): Estimation of the mechanical properties of amorphous metal with a dispersed nano-crystalline particle by molecular dynamics simulation. *CMES: Computer Modeling in Engineering & Sciences*, vol. 10, pp. 187–198.

Matsumoto, R.; Nakagaki, M.; Nakatani, A.; Kitagawa, H. (2005): Molecular-dynamics study on crack growth behavior relevant to crystal nucleation in amorphous metal. *CMES: Computer Modeling in Engineering & Sciences*, vol. 9, pp. 75–84.

Nagahiro, S.; Kawano, S.; Kotera, H. (2007): Separation of long DNA chains using a nonuniform electric field: A numerical study. *Phys. Rev. E*, vol. 75, pp. 011902.

Nishimura, K.; Miyazaki, N. (2001): Molecular dynamics simulation of crack propagation in polycrystalline material. *CMES: Computer Modeling in Engineering & Sciences*, vol. 2, pp. 143–154.

Onufriev, A.; Bashford, D.; Case, D. A. (2004): Exploring protein native states and large-scale conformational changes with a modified generalized born model. *Proteins*, vol. 55, pp. 383–394.

Rief, M.; Clausen-Schaumann, H.; Gaub, H. E. (1999): Sequence-dependent mechanics of single DNA molecules. *Nature Struct. Mol. Biol.*, vol. 6, pp. 346–349.

Shimizu, N.; Kawano, S.; Tachikawa, M. (2006): Electron correlated and density functional studies on hydrogen-bonded proton transfer in adenine-thymine base pair of DNA. *J. Mol. Struct.*, vol. 735-736, pp. 243–248.

Shintaku, H.; Kuwabara, T.; Kawano, S.; Suzuki, T.; Kanno, I.; Kotera, H. (2007): Micro cell encapsulation and its hydrogel-beads production using microfluidic device. *Microsyst. Technol.*, vol. 13, pp. 951–958.

Shintaku, H.; Okitsu, T.; Kawano, S.; Matsumoto, S.; Suzuki, T.; Kanno, I.; Kotera, H. (2008): Effects of fluid dynamic stress on fracturing of cell-aggregated tissue during purification for islets of langerhans transplantation. *J. Phys. D: Appl. Phys.*, vol. 41, pp. 115507.

Sides, P. J.; Faruqui, D.; Gellman, A. J. (2009): Dynamics of charging of muscovite mica: measurement and modeling. *Langmuir*, vol. 25, pp. 1475–1481.

Sotomayor, M.; Schulten, K. (2007): Single-molecule experiments in vitro and in silico. *Science*, vol. 316, pp. 1144–1148.

- Srivastava, D.; Atluri, S. N.** (2002): Computational nanotechnology: A current perspective. *CMES: Computer Modeling in Engineering & Sciences*, vol. 3, pp. 531–538.
- Tanaka, H.; Nishikawa, Y.** (2005): Viscoelastic phase separation of protein solutions. *Phys. Rev. Lett.*, vol. 95, pp. 078103 (4 pages).
- Tanaka, S.; Cai, L.; Tabata, H.; Kawai, T.** (2001): Formation of two-dimensional network structure of DNA molecules on si substrate. *Jpn. J. Appl. Phys.*, vol. 40, pp. L407–L409.
- Tanaka, S.; Maeda, Y.; Cai, L.; Tabata, H.; Kawai, T.** (2001): Formation of two dimensional network structure of DNA molecules on highly ordered pyrolytic graphite surface. *Jpn. J. Appl. Phys.*, vol. 40, pp. 4217–4220.
- Terawaki, A.; Otsuka, Y.; Lee, H.; Matsumoto, T.; Tanaka, H.; Kawai, T.** (2005): Conductance measurement of a DNA network in nanoscale by point contact current imaging atomic force microscopy. *Appl. Phys. Lett.*, vol. 86, pp. 113901 (3 pages).
- Tolman, S.; Meakin, P.** (1989): Off-lattice and hypercubic-lattice models for diffusion-limited aggregation in dimensionalities 2-8. *Phys. Rev. A*, vol. 40, pp. 428–437.
- Witten, T. A.; Sander, L. M.** (1981): Diffusion-limited aggregation, a kinetic critical phenomenon. *Phys. Rev. Lett.*, vol. 47, pp. 1400–1403.
- Wu, A.; Li, Z.; Wang, E.** (2004): DNA network structures on various solid substrates investigated by atomic force microscopy. *Anal. Sci.*, vol. 20, pp. 1083–1086.

